Mathematical Description of the Stress-Strain Behavior of Filled Binders

FRED H. BROCK, *Solid Propellant Research Operations of the Solid Rocket Plant, Aerojet-General Corporation, Azusa, California*

Introduction

Much of the theoretical work on elasticity has been concerned with unfilled bodies, ranging from those with a high tensile and low elongation at break, such as metals, to those with a relatively low tensile and high elongation at break, such as organic rubbers.   In the analyses of the stress-strain data of highly filled systems, the infinitesimal theory of elasticity is used very frequently, although it has the inherent disadvantage that it is applicable for small strains only and that it was developed for homogeneous or unfilled bodies and not for heterogeneous or filled systems.   In view of the large strains undergone by filled binders, in this investigation the concepts of the finite elastic theory were applied to these systems.   Although this theory has been used by Rivlin[1] to explain the mechanical behavior of binders, its application to filled binders is a new approach.   This paper describes the results of a phenomenological study in the analysis of stress-strain data by means of the finite elastic theory.

Theoretical Aspects

Strain Invariants

In the theory of finite elasticity three strain invariants are used that are independent of the coordinate axes and are functions of even powers of the principal elongation ratios:

$$I_1 = \lambda_1{}^2 + \lambda_2{}^2 + \lambda_3{}^2 \tag{1}$$

$$I_2 = \lambda_1{}^2\lambda_2{}^2 + \lambda_2{}^2\lambda_3{}^2 + \lambda_1{}^2\lambda_3{}^2 \tag{2}$$

$$I_3 = \lambda_1{}^2\lambda_2{}^2\lambda_3{}^2 \tag{3}$$

where the λ_i are the principal extension ratios.

For incompressible bodies, $I_3 = 1$.   It is well known that voids are formed on straining filled binders, so that the value of I_3 will not be equal to unity and that Poisson's ratio will not be equal to 0.5.

If $I_3 = 1$, then for uniaxial strain:

$$\lambda_1 = \lambda \tag{4}$$

$$\lambda_2 = \lambda_3 = 1/\lambda^{1/2} \tag{5}$$

where λ is the elongation ratio along the axis of strain. Substitution of eqs. (4) and (5) into eqs. (1) and (2) shows that

$$I_1 = \lambda^2 + 2/\lambda \tag{6}$$

$$\text{and} \quad I_2 = 2\lambda + 1/\lambda^2 \tag{7}$$

In biaxial strain, in which a long specimen is extended in the direction of the shorter axis, so that the length is considered constant, $\lambda_1 = \lambda, \lambda_2 = 1$, $\lambda_3 = 1/\lambda$, so that

$$I_1 = I_2 = \lambda^2 + 1/\lambda^2 + 1 \tag{8}$$

Stored-Energy Function

In terms of the strain invariants, the stored-energy function W, or the energy of deformation per unit volume, is expressed by

$$W = W(I_1, I_2, I_3) \tag{9}$$

Since $W = 0$ for the undeformed body (i.e., $\lambda_i = 1$, so that $I_1 = I_2 = 3$), a general expression of W for incompressible bodies, for which $I_3 = 1$, will involve terms in $(I_1 - 3)$ and $(I_2 - 3)$, i.e.,

$$W = \sum_{i=0}^{\infty} \sum_{j=0}^{\infty} (I_1 - 3)^i (I_2 - 3)^j \tag{10}$$

This expression reduces to the Mooney equation when $i = 1, j = 0$ and $i = 0, j = 1$:

$$W = C_1(I_1 - 3) + C_2(I_2 - 3) \tag{11}$$

When $C_2 = 0$, eq. (11) reduces to the relationship given by the kinetic theory of elasticity.

The stored-energy function per unit volume is determined by:

$$W = \int_{\lambda_i} \sigma(\lambda_i) d\lambda_i \tag{12}$$

where $\sigma(\lambda_i)$ is the stress.

Hence, in the absence of voids, the value of W is given by the area under the experimental stress-strain curve.

Experimental Procedure

Uniaxial tensile testing was performed with standard Instron specimens with a gage length of 2.7 in. The biaxial specimens were 7 in. long, 0.25 in. thick, and 0.5 in. in gage length. The instruments used were an Instron tensile tester (Model TTC) for low rates (crosshead speeds of 0.05 to 20 in./min.) and an Alinco high-rate tester (Model 625A) for high rates (crosshead speeds of 500 to 5,000 in./min.).

Data Analyses

It was realized that voids are formed on straining filled binders, and that consequently the strain invariants and the stored-energy function would

have to be corrected to take volume changes into account. However, pseudostrain invariants were defined, which are expressed by the identical functions of λ as the strain invariants when no volume changes take place, as given by eqs. (6), (7), and (8). These pseudostrain invariants were designated as Q_{ij}, where the first subscript indicates the subscript of the I invariant to which it is related, and the second subscript indicates the type of strain, i.e., 1 for uniaxial and 2 for biaxial. Hence, the definition of the Q_{ij}'s in terms of the λ's for uniaxial strain are:

$$Q_{11} = \lambda^2 + 2/\lambda \tag{13}$$

$$Q_{21} = 2\lambda + 1/\lambda^2 \tag{14}$$

and for biaxial strain:

$$Q_{12} = Q_{22} = \lambda^2 + 1/\lambda^2 + 1 \tag{15}$$

It may be noted that if volume changes are taken into account, so that

$$I_3^{1/2} = V/V_0 \neq 1 \tag{16}$$

where V is the volume at a given strain level and V_0 is the original volume, it follows from eqs. (1), (2), and (3) that for uniaxial strain,

$$I_1 = \lambda^2 + (2/\lambda)(V/V_0) \tag{17}$$

and for biaxial strain

$$I_1 = \lambda^2 + (1/\lambda^2)(V/V_0)^2 + 1 \tag{18}$$

The value of V/V_0 is essentially unity at small values of λ, but increases with increasing λ. However, the coefficient of V/V_0 in uniaxial strain, or of $(V/V_0)^2$ in biaxial strain, decreases as $1/\lambda$ or as $1/\lambda^2$, respectively, so that the contribution of the volume correction term to the value of I_1 is not great even at high elongations; i.e., Q and I are practically equal unless large volume changes occur at low elongations.

Application of PseudoStrain Invariants

Values of the stored-energy function, assumed to be equal to the area under the stress-strain curve, were determined for both uniaxial and biaxial testing data covering a wide range of temperature strain rate and type of filled system. The values of W were plotted against $(Q_{ij} - 3)$. It was found that W was represented by the general equation

$$W = A[1 - \exp\{-B(Q_{ij} - 3)\}] \tag{19}$$

where A and B are constants. A is the value which W is approaching exponentially and B is a measure of the rate of increase of W. A further discussion of the nature and role of these constants is presented below. Owing to the almost linear numerical relationship between I_1 and I_2 in uniaxial strain, W is expressible by similar functions of Q_{21} and Q_{11}. However, only the expression involving Q_{11} will be discussed, since at small extension ratios

or for small B values, it reduces to the equation given by the kinetic theory of elasticity:

$$W = AB(Q_{1j} - 3) \tag{20}$$

That is, W is a linear function of the pseudostrain invariants, which is identical to eq. (11) for $C_2 = 0$. Such linear plots have been observed in this investigation. From the definition of W it follows that

$$dW/d\lambda = \sigma(\lambda) \tag{21}$$

Substitution of eq. (19) into eq. (21) and expressing Q_{11} in terms of λ yields the uniaxial stress-strain equation

$$\sigma(\lambda) = 2AB(\lambda - 1/\lambda^2) \exp \{-B(\lambda^2 + 2/\lambda - 3)\} \tag{22}$$

whereas the biaxial stress-strain equation is given by

$$\sigma(\lambda) = 2AB(\lambda - 1/\lambda^3) \exp \{-B(\lambda^2 + 1/\lambda^2 - 2)\} \tag{23}$$

The initial modulus for the uniaxial strain is obtained from eq. (22):

$$d\sigma(\lambda)/d\lambda|_{\lambda=1} = 6AB \tag{24}$$

These results are to be compared with those obtained from eq. (11), when $C_2 = 0$, from which it follows that

$$\sigma(\lambda) = 2C_1 (\lambda - 1/\lambda^2) \tag{25}$$

and $d\sigma(\lambda)/d\lambda|_{\lambda=1} = 6C_1$

At small strains or small B values, eq. (22) becomes identical with eq. (25).

Differentiation of eq. (23) shows that the initial modulus for biaxial strain is given by

$$d\sigma(\lambda)/d\lambda|_{\lambda=1} = 8AB \tag{27}$$

When W is a linear function of Q_{ij}, as in eq. (20), the slope is equal to AB, so that the modulus is equal to 6 times the slope in uniaxial strain and to 8 times the slope in biaxial strain.

At the maximum of the biaxial stress-strain curve

$$B = \lambda_m{}^2 (\lambda_m{}^4 + 3)/[2 (\lambda_m{}^4 - 1)^2] \tag{28}$$

where λ_m is the extension ratio at the maximum stress. At the maximum of the uniaxial curve

$$B = \lambda_m (\lambda_m{}^3 + 2)/[2 (\lambda_m{}^3 - 1)^2] \tag{29}$$

When $\lambda \gg 1$, both eqs. (28) and (29) reduce to

$$B \approx 1/2\lambda_m{}^2 \tag{30}$$

It is seen that λ_m is independent of A, and dependent only on B. Conversely, the value of B may be computed from λ_m and then substituted in eqs. (24) or (27) to solve for A. However, the value of B obtained by this

method is not as accurate as that obtained by the method described below, since it is determined by a function involving only one specific value of λ instead of those in the whole range of the stress-strain curve and, in addition, this function is very sensitive to small errors in λ_m.

Calculation of A and B

The value of A was determined by trial and error, by choosing reasonable values of A and plotting log $(1 - W/A)$ against $(Q_{ij} - 3)$ until the resulting plot was linear. Generally, the value of A could be found in one or two trials. The value of B was calculated from the slope of this linear plot. In several graphs, small deviations from linearity were observed at very low elongations and also the semilog plots had an intercept, so that eq. (19) became

$$W = A\,[1 - C \exp\,\{-B(Q_{ij} - 3)\}\,]\qquad(31)$$

where C is the value of the intercept, generally ranging from 0.95 to 1.02. These intercepts are in many cases due probably to experimental errors caused by slippage of the specimen in the Instron and to the fact that the area under the initial portion of the curve is small. In other cases, C deviates from unity when the stress-strain curve has a very steep initial slope followed by a markedly different slope. The effect of C on eqs. (24) and (27) is to equate the computed modulus to $6ABC$ and $8ABC$, respectively.

Another method of computing these constants involves the use of the stress-strain equations, eqs. (22) or (23). For biaxial data, a plot of ln $\sigma/(\lambda - 1/\lambda^3)$ vs. $(Q_{12} - 3)$ would have a slope of $-B$ and an intercept of ln $2AB$, assuming $C = 1$. However, this plot is extremely sensitive to experimental errors in the initial portion of the graph, since small differences are involved in the denominator of the ln term, so that too much weight is placed on the data at higher extensions. Therefore, this method of obtaining the constants A, B, and C is not as satisfactory as the method outlined previously.

Typical graphs used in these computations are presented in Figures 1, 2, and 3, which show, respectively, a typical biaxial stress-strain curve, the corresponding plot of W vs. $(Q_{12} - 3)$, and the semilog plot of $(1 - W/A)$ vs. $(Q_{12} - 3)$.

Discussion of Experimental Results

In Table I are presented the biaxial data of two filled binders, designated as systems I and II, respectively. In order to compare the uniaxial and biaxial data of specimens obtained from the same batches, a 10 lb. mix of system III, containing 59 wt.-% salt and 15% aluminum powder of 15μ dia and a 10 lb. mix of system IV, containing 65 wt.-% glass beads of 114 μ dia and 84 μ dia were prepared. Both uniaxial and biaxial specimens were tested over a wide range of strain rate and temperature, i.e., 0.1–10,000 min.$^{-1}$ and 40–110°F. for the biaxial tests, and 0.074–740 min.$^{-1}$

and -40–$110°F$. for the uniaxial tests.   The resulting data are listed in Tables II and III.

Included in the tables are columns of the extension ratios at break, λ_b, the work to break, W_b (assuming incompressibility), the modulus calcu-
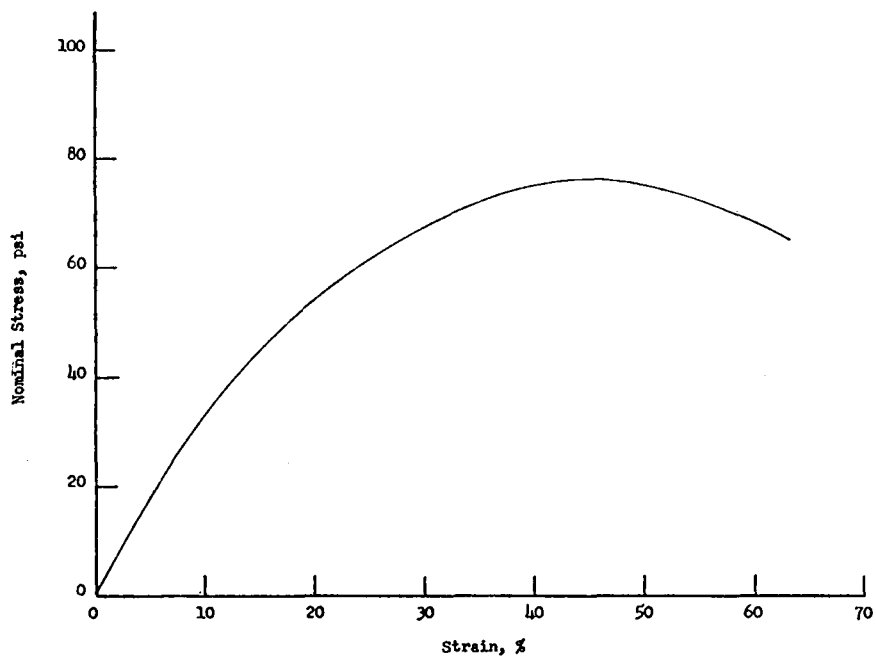

Fig. 1. Biaxial stress-strain curve for salt-filled system II.   Test temperature $110°F.$, strain rate 20 min.$^{-1}$.

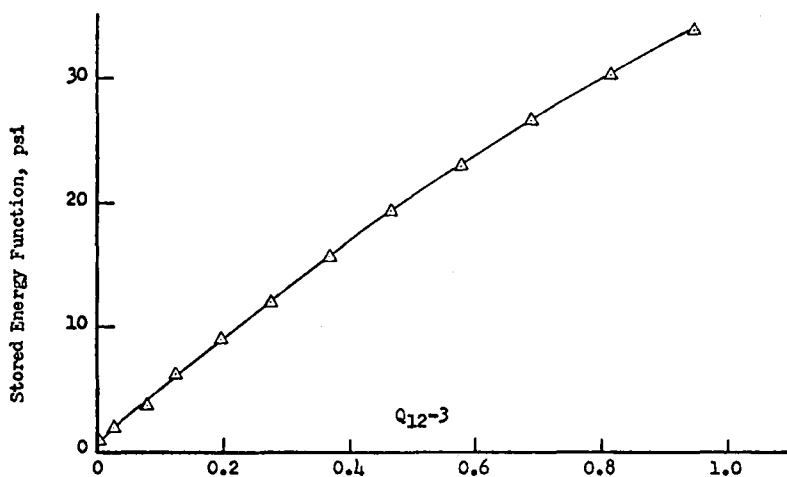Fig. 2. Plot of stored-energy function against Q_{12} -3 for salt-filled system II. Test temperature $110°F.$, strain rate 20 min.$^{-1}$.
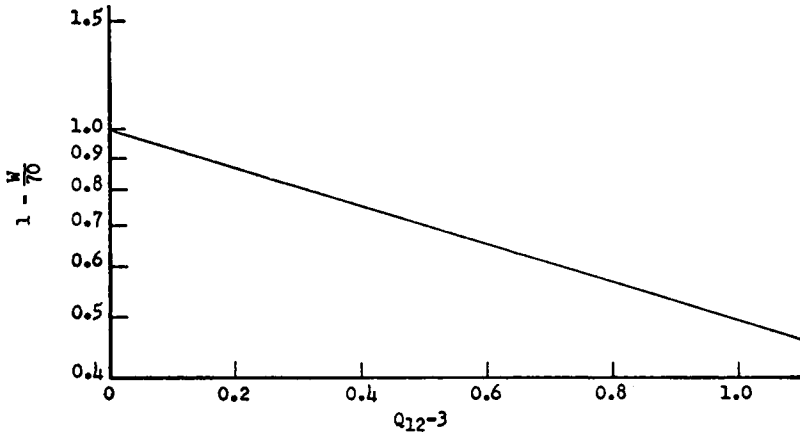
Fig. 3. Graph for determination of constants A and B for salt-filled system II. Test temperature, 110°F., strain rate 20 min.$^{-1}$.

lated from the slope of the stress-strain curves, and the computed values of the constants A, B, and C. The slopes of the linear plots of W vs. $(Q_{1j} - 3)$ are given in the column "Linear slopes." Values of the initial moduli E, calculated by use of the constants A, B, C, or from the values under "Linear slopes" by means of eq. (24) or (27), are given in the last column.

TABLE I
Reduced Biaxial Stress-Strain Data of Systems I and II

Temp., °F.	ϵ, min.$^{-1}$	λ_b	W_b, psi	A, psi	B	C	W_b/A
			System I				
20	20	2.82	913.10	1200	0.22	0.94	0.76
	40	1.62	322.10	450	1.18	0.94	0.72
60	20	4.02	389.55	500	0.10	0.91	0.78
	40	5.31	649.50	800	0.056	0.88	0.81
80	20	3.49	253.49	280	0.19	0.94	0.90
	40	3.30	243.04	300	0.17	0.95	0.81
	200	2.90	312.00	420	0.20	0.96	0.74
	1,000	2.50	375.58	500	0.29	0.91	0.75
	2,000	1.80	288.48	350	0.80	0.96	0.80
	10,000	1.68	261.32	340	1.17	0.96	0.82
110	20	2.50	128.15	180	0.28	0.97	0.71
	40	2.66	134.86	180	0.26	0.96	0.75
			System II				
40	40	1.83	131.91	220	0.53	0.96	0.60
80	20	1.73	53.87	80	0.82	1.00	0.67
	40	1.84	67.82	100	0.65	1.00	0.68
100	20	1.64	36.47	70	0.71	1.00	0.52
	40	1.61	44.27	80	0.82	1.00	0.55

TABLE II
Reduced Stress–Strain Data of System III

Temp., °F.	$\dot{\epsilon}$, min.$^{-1}$	λ_b, %	W_b	E, psi	A	B	C	W_b/A	Linear slope	E (calcd.)
				Biaxial						
40	0.1	12.9	6.34	994	12	13.3	1.02	0.53	—	1300
40	740	56	205	2941	260	1.8	1.00	0.79	—	3740
40	10,000	54	251	3500	350	1.65	1.02	0.72	—	4710
80	0.1	11.5	4.51	742	—	—	—	—	97.5	780
80	0.1	8.5	3.29	1010	—	—	—	—	127	1020
80	10	11.0	8.53	1705	—	—	—	—	199	1590
80	10	10.7	7.50	1370	—	—	—	—	189	1510
80	740	32.0	92.5	4000	120	4.56	1.00	0.77	—	4380
80	2000	33.0	107.5	2900	200	2.37	1.00	0.54	—	3790
80	2000	28.0	108	5100	160	4.47	1.00	0.68	—	5720
80	10,000	36.0	133	3000	200	2.88	1.03	0.67	—	4750
110	0.1	9.6	4.6	1100	—	—	—	—	137	1090
110	0.1	9.52	4.1	1000	—	—	—	—	124	992
110	10,000	58.0	125	1680	150	1.80	1.02	0.83	—	2200
				Uniaxial						
−40	740	9.26	106	55,000	130	66.0	1.00	0.82	—	51,000
80	0.074	34.6	14.8	405	22	3.72	1.00	0.67	—	491
80	7.4	26.9	28.5	1990	35	8.56	1.00	0.81	—	1800
80	740	35.2	67.5	3090	80	5.68	1.00	0.84	—	2730
110	0.074	12.6	6.9	948	—	—	—	—	157	942

TABLE III
Reduced Stress–Strain Data of System IV, Containing 65 vol.-% Glass Beads

Temp., °F.	$\dot{\epsilon}$, min.$^{-1}$	λ_b, %	W_b	E, psi	A	B	C	W_b/A	Linear slope	E (calcd.)
				Biaxial						
40	0.1	12.2	4.00	618	—	—	—	—	79.0	632
40	740	22.0	78.7	3650	—	—	—	—	481	3850
40	10,000	22.0	86.8	4480	—	—	—	—	585	4680
80	0.1	7.52	1.72	852	2.5	53.3	1.02	0.69	—	1090
80	10	7.83	3.30	1450	—	—	—	—	145	1160
80	740	54.0	66.0	1070	80	1.85	1.00	0.83	—	1180
80	2,000	28.0	85.5	3740	120	4.84	1.01	0.71	—	4690
80	10,000	28.0	83.0	3200	120	4.68	1.02	0.69	—	4580
110	0.1	6.12	1.06	620	—	—	—	—	78.6	629
110	10,000	36.0	63.8	2640	80	3.69	1.02	0.80	—	2410
				Uniaxial						
−40	740	7.41	116.6	53,600	180	59.7	1.02	0.65	—	66,000
40	740	14.4	30.7	6,100	40	24.7	1.02	0.77	—	6050
80	0.074	14.3	3.07	355	—	—	—	—	60.4	362
80	7.4	12.6	7.75	1930	10	32.5	1.01	0.78	—	1970
80	740	20.0	23.8	2430	30	13.9	1.00	0.80	—	2490
110	0.074	5.48	1.05	940	—	—	—	—	146	876

At a given temperature, the stored energy to break, W_b, and A generally increase with increasing strain rate in both the uniaxial and biaxial tests. However, the biaxial data in Table I for system I at 80° show that both W and A go through a maximum owing to the relative values of low tensile and high elongations at low strain rates, and high tensile and low elongations at high strain rates.

A few comments may be made about the effect of variations of test conditions on the value of W_b.

The data in Table II for system III show that at 80° at low strain rates the value of W_b in biaxial strain is lower than that in uniaxial strain, whereas at a high strain rate the converse is true.   At low strain rates the values of W_b in biaxial tests are in a ratio of 0.3 to those in the uniaxial tests, whereas at 110° this ratio increases to approximately 0.7.   For the glass bead-filled binder, system IV, (Table III) these ratios are approximately 0.5 and 1, respectively.   However, at a strain rate of 740 min.$^{-1}$ at 80°, the values of W_b and A for system III in biaxial tests are approximately 50% greater than those in the uniaxial test, whereas for system IV at 40 and 80°, the corresponding increases are about 170%.

Failure Criterion

An inspection of the values of W_b and A in Tables I–III shows that, within experimental error, the ratio W_b/A, also listed in the tables, is a constant whose value generally lies between 0.7 and 0.8, irrespective of the filled system, strain rate, and temperature, and which holds for both biaxial and uniaxial data.

This constancy, which is an important relationship in that it helps to define completely the stress-strain curve for a filled system (including a good prediction of the stress and strain at break), may also be deduced from other considerations and used for drawing further conclusions and useful correlations from the stress-strain data.

For simplicity, a quantity k will be defined as

$$k \equiv -\ln (1 - W_b/A) \tag{32}$$

It will now be shown that k, and hence W_b/A, is indeed a constant for the available data.

First the data will be discussed for which W is an exponential function of $Q_{\eta j}$, i.e. the nonlinear data, and then the data for which W is a linear function of $Q_{\eta j}$, i.e. the linear data.

Failure in Biaxial Strain (Nonlinear Data)

When W obeys eq. (19), i.e., is nonlinear, it follows from eqs. (19) and (32) that

$$\lambda_b = [\{2 + k/B + (4k/B + k^2/B^2)^{1/2}\}/2]^{1/2} \tag{33}$$

Two cases are of interest:

$$(1) \text{ When } B < k, \text{ then } B \approx k/(\lambda_b{}^2 - 2) \qquad (34)$$

$$(2) \text{ When } B > k, \text{ then } B \approx k/(\lambda_b{}^2 - 1)^2 \qquad (35)$$

Equations (34) and (35) may also be derived from eqs. (19) and (32) assuming λ_b to be large, and small, respectively. However, when $B >> k$, then $\lambda_b \approx 1$; i.e., failure occurs at very low extensions. This conclusion also follows from the form of eq. (19).

Failure in Uniaxial Strain (Nonlinear Data)

At failure in uniaxial strain, λ_b is the solution of the equation

$$\lambda_b{}^3 - \lambda_b (3 + k/B) + 2 = 0 \qquad (36)$$

$$\text{i.e.,} \qquad \lambda_b = (2/3^{1/2})(3 + k/B)^{1/2} \cos (\phi/3) \qquad (37)$$

$$\text{where} \qquad \cos \phi = -\ [3/(3 + k/B)]^{3/2} \qquad (38)$$

Again, as in the biaxial case, two limiting conditions may be considered:
(1) When $B < k$, it follows from eqs. (37) and (38) or from eq. (36) that

$$\lambda_b \approx (3 + k/B)^{1/2} \qquad (39)$$

(2) When $B > k$, it follows, by expanding $\cos \phi$ in a Taylor's series about π and then by expanding $\cos (\phi/3)$ about $\pi/3$, that

$$\lambda_b \approx 1 + (k/3B)^{1/2} \qquad (40)$$

The same result is obtained from eq. (36) assuming λ_b to be small.

When $B >> k$, then $\lambda_b \approx 1$ and the same comments apply as those for the corresponding biaxial solution.

It should be noted that eqs. (34) and (39) are similar for $\lambda_b >> 1$.

Failure in Biaxial and Uniaxial Strain (Linear Data)

The relationships shown in eqs. (35) and (40) provide a method of including those data when W is a linear function Q_{Tj}. If it is assumed that the constancy of W_b/A holds for these data, it follows from the values of W_b and of the "Linear slope" column in Tables II and III that $B > k$ for the linear data.

Designating the value of the linear slope as s, and substituting for the value of A in the expression for s from eq. (20) shows that

$$B = (1 - e^{-k})(s/W_b) \qquad (41)$$

Substitution of this expression for B in eq. (35) shows that for failure in biaxial strain

$$\lambda_b{}^2 = 1 + (k/1 - e^{-k})^{1/2} (W_b/s)^{1/2} \qquad (42)$$

while at failure in uniaxial strain, it follows from eqs. (40) and (41) that

$$\lambda_b = 1 + [k/3(1 - e^{-k})]^{1/2} (W_b/s)^{1/2} \qquad (43)$$

In order to present the linear and nonlinear data for which $B > k$ in a unified form—that is, without using the values of A and B of the nonlinear data to compute the values of s so that similar experimental data are used in treating the linear and nonlinear data—use is made of eqs. (24) and (27) to modify eqs. (43) and (42), respectively. It follows that for the biaxial data:

$$\lambda_b{}^2 = 1 + (k/1 - e^{-k})^{1/2} (8W_b/E)^{1/2} \qquad (44)$$

while for the uniaxial data

$$\lambda_b = 1 + (k/3(1 - e^{-k}))^{1/2} (6W_b/E)^{1/2} \qquad (45)$$

where E is Young's modulus obtained as the initial tangent of the stress-strain curve.

Determination of k and Discussion of Results

The above relationships, eqs. (34), (35), (39), (40), (44), and (45) suggest graphical methods of determining whether k is a constant in any of the above series and whether its value is independent of the series. For the purpose of determining the limits of B that determine the ranges in which these equations are applicable, k was chosen as 1.61, corresponding to a value of W_b/A of 0.8. (Other relationships, that involve only the stress at break σ_b, λ_b, E and k, result from the combination of eqs. (32) and (19) with eqs. (22) and (24) for the uniaxial data, and with eqs. (23) and (27) for the biaxial data, respectively.)

The following table summarizes the types of plots that were constructed, the corresponding figure numbers and the results. No data were available for use with eq. (39).

Stress-strain data	Fig. no.	Plots	Slope	Obsd. slope	W_b/A, calcd.
Biaxial $B < k$	4	$\lambda_b{}^2$ vs. $1/B$	k	1.52	0.78
Biaxial $B > k$	5	$\lambda_b{}^2$ vs. $1/B^{1/2}$	$k^{1/2}$	1.36	0.84
Biaxial linear and nonlinear	6	$\lambda_b{}^2$ vs. $(8W_b/E)^{1/2}$	$[k/(1 - e^{-k})]^{1/2}$	1.42	0.80
Uniaxial $B > k$	7	λ_b vs. $1/B^{1/2}$	$(k/3)^{1/2}$	0.72	0.79
Uniaxial linear and nonlinear	8	λ_b vs. $(6W_b/E)^{1/2}$	$[k/3(1 - e^{-k})]^{1/2}$	0.77	0.73

Inspection of Figures 4–8 shows that within experimental error good linearity is obtained. When $B > k$, λ_b is small, so that experimental errors are quite important in these plots. The points that have large deviations, also do not fall on a smooth curve of B vs. λ_b.

Several conclusions may be reached from these data.

(1) Since the plots are linear and the slopes are functions of k only as listed in the above table, the value of k is constant in all series. From the observed values of these slopes, k and hence, W_b/A were computed by means of eq. (32). As seen in the last column of the table, this ratio has

essentially a constant value of 0.8, which is independent of the type of strain, strain rate, λ_b, W_b, or E.

(2) These graphical methods provide an independent means of determining W_b/A, as is shown in the following brief analysis. For the nonlinear data, the plots showed that
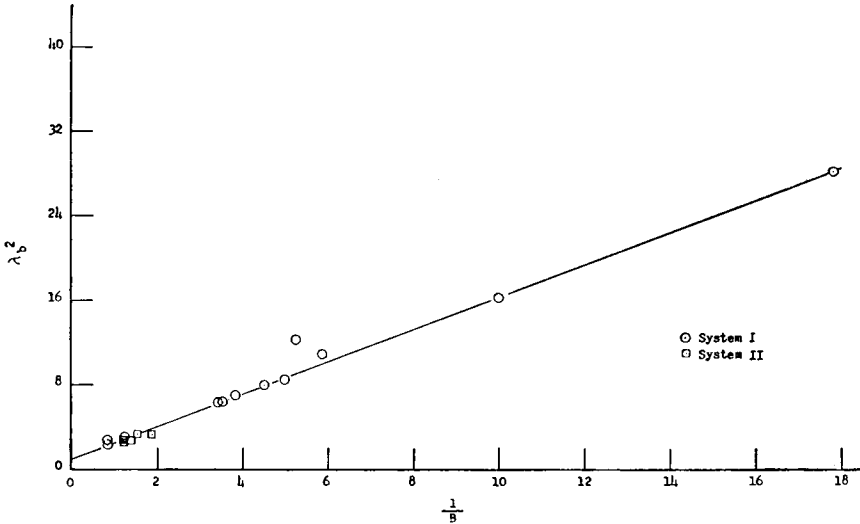
$$k = (B, \lambda_b) \tag{46}$$

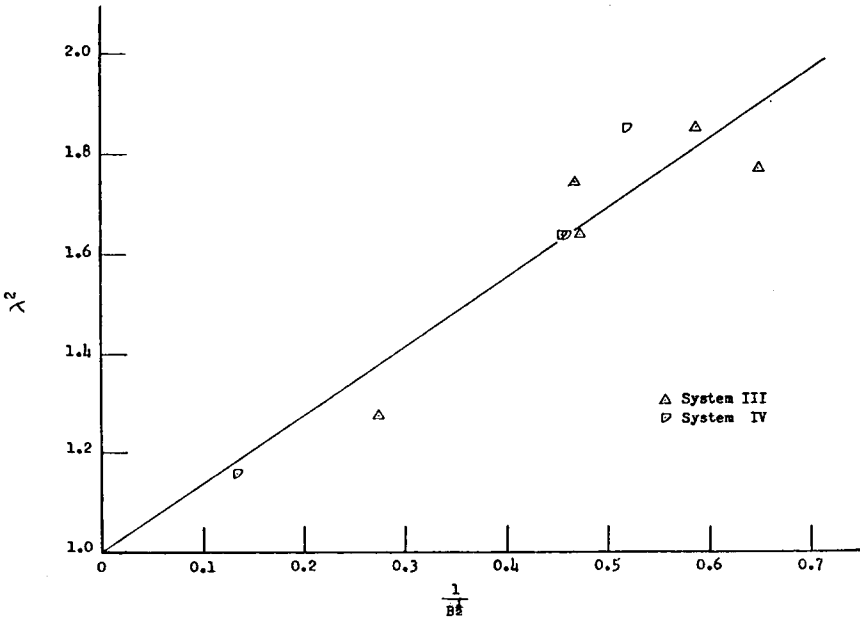Fig. 4. Determination of k from biaxial data when $B < 1.61$.
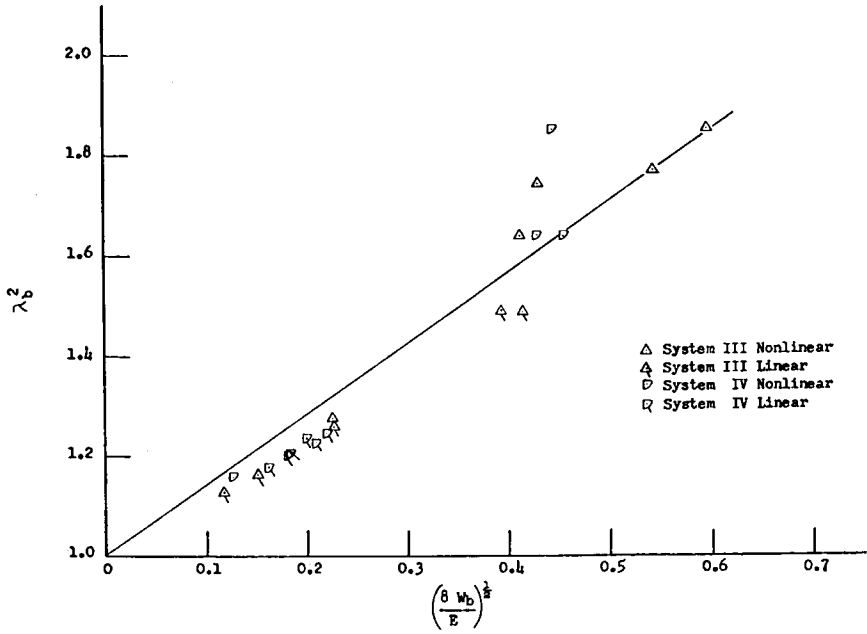

Fig. 5. Determination of k from biaxial data when $B > 1.61$.

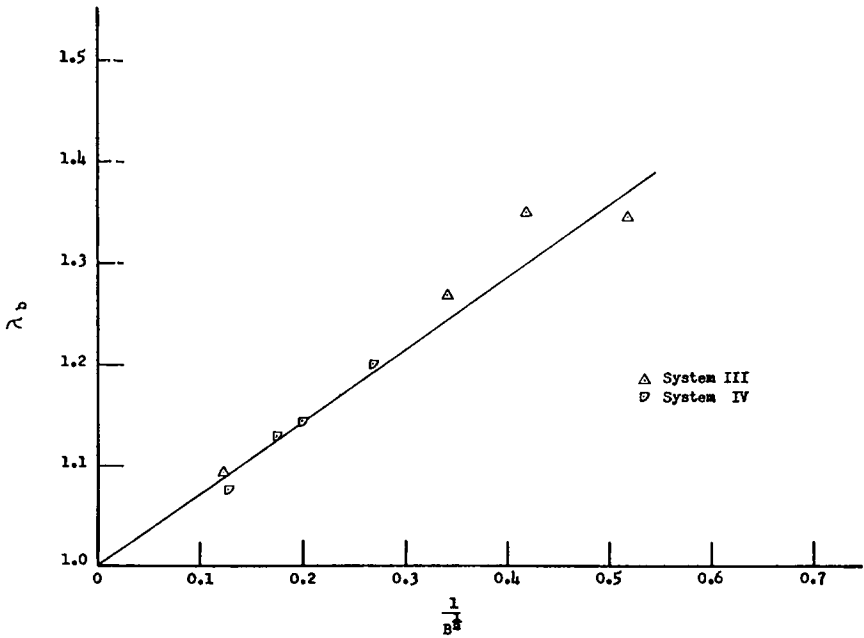Fig. 6. Determination of k from linear and nonlinear biaxial data when $B > 1.61$.

Fig. 7. Determination of k from uniaxial data when $B > 1.61$.

That is, k was calculated from the set containing values of B and λ_b only. Since B can also be calculated from λ_m, it follows that

$$k = (\lambda_m, \lambda_b) \tag{47}$$

When k was computed from the plots with both the linear and nonlinear data,

$$k = (W_b, E, \lambda_b) \tag{48}$$
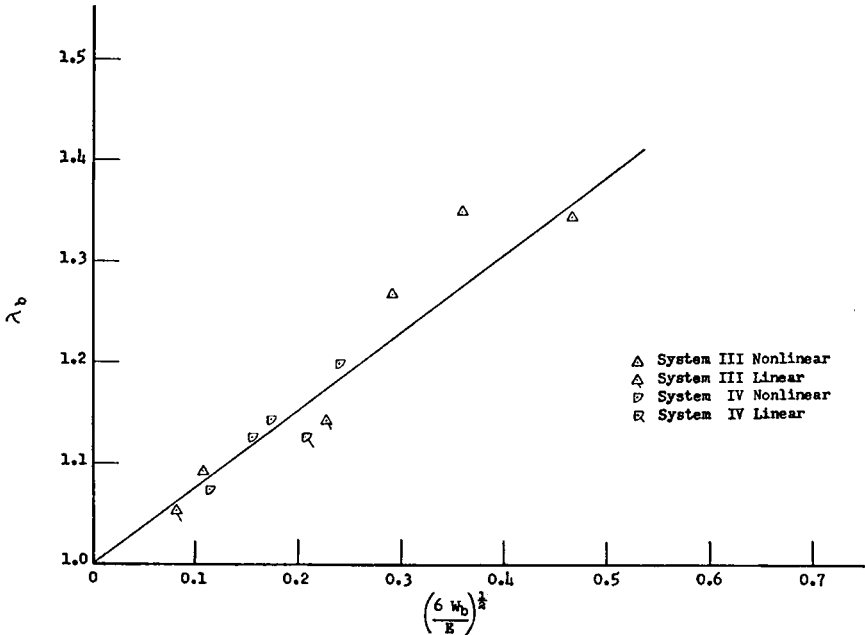
and

$$k = (\sigma_b, E, \lambda_b) \tag{49}$$

Fig. 8. Determination of k from linear and nonlinear uniaxial data when $B > 1.61$.

In contrast, the values of W_b/A as listed in Tables I, II, and III were determined from the stress-strain data, so that by this method

$$k = (\sigma, \lambda) \tag{50}$$

Hence, the data from which k is determined by these graphical methods are independent of the data used to compute directly the W_b/A values, so that the graphical procedures provide an independent check on the value and constancy of W_b/A.

(*3*) From a phenomenological point of view and the value of the constant ratio of W_b/A, it may be concluded that A is the amount of energy

required to cause an infinite elongation of the filled system, but the system is able to absorb only 80% of that energy before it fails.

(4) The linear data are consistent with eq. (19) not only in that they represent the limiting case when λ_b is small, but that they also appear to obey the same failure criterion.

(5) The values of λ_m and λ_b are dependent on B and not on A. Hence, in terms of the proposed equation, the modulus may be considered to consist of two components: a strain component B and an energy component A.

(6) Since λ_m and λ_b are related by eqs. (28) and (33) in biaxial strain, and by eqs. (29) and (37) in uniaxial strain, it follows that if failure occurs at λ_m, then for a given type of strain, this mode of failure will occur at the same extension ratio in systems with the same k value.

Reference

1. Rivlin, R. S., *Phil. Trans. Roy. Soc. London, Ser.*, A, **241**, 379 (1948).

Synopsis

The result of a phenomenological study in the analysis of uniaxial and biaxial tensile behavior of a variety of filled systems is described. A correlation is given that appears to serve as a tensile failure criterion for most of the systems investigated. The stored-energy function W, assumed to be equal to the area under the stress-strain curve, has been found to obey the relation $W = A(1 - \exp\{-B(Q - 3)\})$, where A and B are constants and Q is related to the first or second strain invariant. In general, the total stored energy up to break, divided by A, has a value between 0.7 and 0.8, which appears to be independent of strain rate and temperature. This constancy has also been verified by an independent set of data.

Résumé

Cet article décrit le résultat de l'étude phénoménologique dans l'analyse du comportement à la traction uniaxiale et biaxiale d'une variété de systèmes contenant des charges, et une corrélation qui semble servir de critère à la cassure sous tension pour la plupart des systèmes étudiés. La fonction d'énergie accumulée, W, que l'on suppose mesurée par la surface comprise endessous de la courbe tension-traction, obéit à la relation $W = A(1 - \exp\{-B(Q - 3)\})$ où A et B sont des constantes et Q est lié au premier ou second invariant de la tension. En général l'énergie totale accumulée jusqu'à la rupture, divisée par A, possède une valeur comprise entre 0.7 et 0.8 qui semble ne pas dépendre de la vitesse de tension et de la température. Cette constance a été vérifiée également par une série de données indépendante.

Zusammenfassung

In der vorliegenden Mitteilung wird das Ergebnis einer phänomenologischen Untersuchung der Analyse des uniaxialen und biaxialen Zugverhaltens einer Reihe gefüllter Systeme und eine Korrelation als Zugbeanspruchbarkeitskriterium für die meisten unter-

suchten Systeme beschrieben.   Die Funktion für die gespeicherte Energie, W, die der Fläche unter der Spannungs-Dehnungskurve gleiche gesetzt wird, entspricht der Beziehung $W = A (1 - \exp\{-B(Q-3)\})$, wo A und B Konstante sind und Q zur ersten oder zweiten Verformungsinvarianten in Beziehung steht.   Im allgemeinen besitzt der Quotient aus gespeicherter Gesamtenergie (bis zum Bruch) und A, scheinbar unabhängig von Verformungsgeschwindigkeit und Temperatur, einen Wert zwischen 0,7 und 0,8. Diese Konstanz wurde durch eine unabhängige Reihe von Daten bestätigt.